

Foveal regeneration after resolution of cystoid macular edema without and with internal limiting membrane detachment: presumed role of glial cells for foveal structure stabilization

Andreas Bringmann¹, Martin Karol², Jan Darius Unterlauff¹, Thomas Barth¹, Renate Wiedemann¹, Leon Kohen^{1,2}, Matus Rehak¹, Peter Wiedemann¹

¹Department of Ophthalmology and Eye Hospital, University of Leipzig, Leipzig 04103, Germany

²Helios Klinikum Aue, Aue 08280, Germany

Correspondence to: Peter Wiedemann. Department of Ophthalmology and Eye Hospital, University of Leipzig, Liebigstraße 12, D-04103 Leipzig, Germany. Peter.Wiedemann@medizin.uni-leipzig.de

Received: 2021-03-11 Accepted: 2021-03-29

Abstract

• **AIM:** To document with spectral-domain optical coherence tomography the morphological regeneration of the fovea after resolution of cystoid macular edema (CME) without and with internal limiting membrane (ILM) detachment and to discuss the presumed role of the glial scaffold for foveal structure stabilization.

• **METHODS:** A retrospective case series of 38 eyes of 35 patients is described. Of these, 17 eyes of 16 patients displayed foveal regeneration after resolution of CME, and 6 eyes of 6 patients displayed CME with ILM detachment. Eleven eyes of 9 patients displayed other kinds of foveal and retinal disorders associated with ILM detachment.

• **RESULTS:** The pattern of edematous cyst distribution, with or without a large cyst in the foveola and preferred location of cysts in the inner nuclear layer or Henle fiber layer (HFL), may vary between different eyes with CME or in one eye during different CME episodes. Large cysts in the foveola may be associated with a tractional elevation of the inner foveal layers and the formation of a foveoschisis in the HFL. Edematous cysts are usually not formed in the ganglion cell layer. Eyes with CME and ILM detachment display a schisis between the detached ILM and nerve fiber layer (NFL) which is traversed by Müller cell trunks. ILM detachment was also found in single eyes with myopic traction maculopathy, macular pucker, full-thickness macular holes, outer lamellar holes, and glaucomatous parapapillary retinoschisis, and in 3 eyes with Müller cell

sheen dystrophy (MCSD). As observed in eyes with MCSD, cellophane maculopathy, and macular pucker, respectively, fundus light reflections can be caused by different highly reflective membranes or layers: the thickened and tightened ILM which may or may not be detached from the NFL, the NFL, or idiopathic epiretinal membranes. In eyes with short single or multiple CME episodes, the central fovea regenerated either completely, which included the disappearance of irregularities of the photoreceptor layer lines and the reformation of a fovea externa, or with remaining irregularities of the photoreceptor layer lines.

• **CONCLUSION:** The examples of a complete regeneration of the foveal morphology after transient CME show that the fovea may withstand even large tractional deformations and has a conspicuous capacity of structural regeneration as long as no cell degeneration occurs. It is suggested that the regenerative capacity depends on the integrity of the three-dimensional glial scaffold for foveal structure stabilization composed of Müller cell and astrocyte processes. The glial scaffold may also maintain the retinal structure after loss of most retinal neurons as in late-stage MCSD.

• **KEYWORDS:** fovea; cystoid macular edema; internal limiting membrane detachment; Müller cell sheen dystrophy; Müller glia; astrocytes

DOI:10.18240/ijo.2021.06.06

Citation: Bringmann A, Karol M, Unterlauff JD, Barth T, Wiedemann R, Kohen L, Rehak M, Wiedemann P. Foveal regeneration after resolution of cystoid macular edema without and with internal limiting membrane detachment: presumed role of glial cells for foveal structure stabilization. *Int J Ophthalmol* 2021;14(6):818-833

INTRODUCTION

The fovea is a pitted invagination of the inner retina which overlies an area of densely packed photoreceptors specialized for high acuity vision (fovea externa)^[1]. It is

formed by centrifugal displacement of the inner retinal layers [nerve fiber layer (NFL) to outer plexiform layer (OPL)]; the displacement decreases the number of light-scattering nerve fibers, synapses, and cell bodies and thus increases the transparency of the retinal tissue in the foveal center^[1]. The fovea comprises the foveola (“little fovea”) and the sloping foveal walls and is surrounded by the parafovea, the thickest retinal area with the highest accumulation of neurons.

The shape of the fovea, with absence of inner retinal layers in the foveola, needs particular structural stabilization. Generally, the retina is mechanically stabilized by the macroglial cell network composed of processes of Müller glial cells and astrocytes; neurons do not provide much structural stability^[2]. The structural tissue stabilization is supported by the strands of microtubules and intermediate filaments like vimentin and glial fibrillary acidic protein (GFAP) in Müller cells and astrocytes^[3]. Müller cells and astrocytes are connected by adherent junctions; these junctions are not present between glial cells and neurons or among neurons, with the exception of the tight-like junctions between Müller and photoreceptor cells near and at the external limiting membrane (ELM)^[3-4]. Müller cells are the only type of macroglia in the fovea; astrocytes are located in the NFL and ganglion cell layer (GCL) of the para- and perifovea^[1]. There are two different populations of Müller cells in the fovea: 1) Specialized Müller cells form the so-called Müller cell cone in the foveola^[1,5-7]. The somata and inner processes of these cells constitute the inner layer of the foveola while the outer processes form the stalk of the Müller cell cone which draws vertically through the center of the foveola^[1,7]; 2) Müller cells of the foveal walls have a characteristic z-shape because their outer processes run horizontally or obliquely through the Henle fiber layer (HFL) towards the foveal center; Henle fibers compensate the spatial shift between the inner and outer layers of the foveal tissue and are composed of photoreceptor cell axons surrounded by the outer processes of the Müller cells of the foveal walls^[7].

Cystoid macular edema (CME) is a common cause of visual impairment associated with a multiplicity of retinal ischemic-hypoxic and inflammatory conditions^[8]. The foveola as well as the inner nuclear layer (INL) and HFL of the foveal walls and parafovea are the preferred locations of edematous cysts in CME^[8-11]. The cysts are formed due to dysregulation of the retinal fluid management resulting from vascular leakage and/or impaired fluid clearance through Müller and retinal pigment epithelial (RPE) cells^[10]. Usually, Müller cells clear excess fluid from the inner retinal layers while the RPE clears excess fluid from the subretinal space and the outer retina up to the OPL-HFL interface. Therefore, edematous cysts in the INL may reflect leakage of retinal vessels and dysfunction of Müller cells whereas edematous cysts in the HFL and subretinal

edema may reflect RPE injury^[12]. Edematous cysts in the HFL may expand up to the ELM and may join the cysts in the INL^[11]. Cysts in the foveola may be caused by fluid exudation from leaky vessels which surround the foveal avascular zone in the foveal walls and/or by dysfunction of both the RPE in the foveola and Müller cells of the foveal walls.

Chronic CME often results in severe disruption of the foveal tissue integrity and is a major cause of macular degeneration, especially when photoreceptor cells degenerate or further pathogenic conditions like diabetes contribute to tissue damage. In the present study, we describe using spectral-domain optical coherence tomography (SD-OCT) that transient CME (in contrast to chronic CME) may be followed by a complete regeneration of the foveal morphology associated with the recovery of a high visual acuity. The restoration of the foveal morphology indicates that the fovea may withstand even large deformations and has a conspicuous capacity of structural regeneration as long as no cell degeneration occurs.

We also describe that CME may be associated with a detachment of the internal limiting membrane (ILM) from the NFL. The ILM is composed of the vitreous-facing endfoot membranes of Müller cells and the basal lamina at the inner retinal surface. ILM detachment is often found in highly myopic eyes; the schisis between the ILM and NFL is vertically traversed by Müller cell trunks; the latter differentiates the detached ILM from the posterior vitreous and idiopathic epiretinal membranes (ERM)^[8,13-19]. ILM detachment is also often a component of glaucomatous peripapillary retinoschisis^[20]. In the present study, we describe that (in addition to eyes with CME, myopic traction maculopathy or parapapillary retinoschisis) ILM detachment may also occur in eyes with macular pucker, full-thickness macular holes (FTMH), outer lamellar holes (OLH), and Müller cell sheen dystrophy (MCS). MCS is a degenerative disease characterized by a glistening retinal surface, retinal folds at the level of the ILM, polycystic edema, and schistic cavities in the retinal tissue^[21-23].

SUBJECTS AND METHODS

Ethical Approval The study followed the ethical standards of the 1964 Declaration of Helsinki and its later amendments. The protocol was approved by the Ethics Committee of the Medical Faculty of the University of Leipzig (#143/20-ek). The ethics committee is registered as Institutional Review Board at the Office for Human Research Protections (registration number, IORG0001320/IRB00001750). Oral informed consent was obtained from all patients; participants did not receive a stipend.

This is a retrospective, single-center chart review. We retrospectively reviewed the charts of 90 447 patients who were referred to the Department of Ophthalmology, University of

Leipzig, Germany, between December 2008 and July 2020. We searched for charts which contained SD-OCT images that showed the presence of a CME in the foveal tissue during the examination period (criterion 1). Thereafter, we selected the charts which contained SD-OCT images that showed a regeneration of the foveal morphology after resolution of CME (criterion 2). We found charts of 17 eyes of 16 patients which fulfilled both criteria. We also searched for charts of eyes with CME and ILM detachment and eyes with other kinds of foveal and retinal disorders associated with ILM detachment. We found charts of 6 eyes of 6 patients with CME and ILM detachment and 11 eyes of 9 further patients with ILM detachment; the latter included eyes with myopic traction maculopathy (1 eye of 1 patient), glaucomatous parapapillary retinoschisis (1 eye of 1 patient), macular pucker (1 eye of 1 patient), FTMH (1 eye of 1 patient), OLH (2 eyes of 2 patients), and MCS D (5 eyes of 3 patients). As examples, we included 2 eyes of 2 patients with cellophane maculopathy and 2 eyes of 2 patients with macular pucker and fundus reflections. All patients were Caucasians. Exclusion criteria were orbital trauma, ocular tumor, and poor quality of SD-OCT imaging.

Statistical Analysis Horizontal or radial scans of the macula were recorded with SD-OCT (Spectralis, Heidelberg Engineering, Heidelberg, Germany). Fundus images were recorded with the Nidek AFC-230 camera (Nidek Co., Ltd., Aichi, Japan). Best-corrected visual acuity (BCVA) was determined using Snellen charts and is given in decimal units. Data are given in means±SD. Statistical analysis was performed using Prism (Graphpad Software, San Diego, CA, USA). Significant differences were evaluated with the non-parametric Mann-Whitney *U* test, and were accepted at $P<0.05$.

RESULTS

Foveal Regeneration After Resolution of Cystoid Macular Edema Figure 1A-1G shows examples of the morphological regeneration of the fovea after resolution of CME in 7 eyes of 7 patients (3 women, 4 men; mean±SD age, 59.4±16.8y; range 29-85y). Five eyes suffered from branch retinal vein occlusion (BRVO; Figure 1A, 1C, 1D, 1F, 1G), one from uveitis (Figure 1B), and one from Irvine-Gass syndrome (Figure 1E). The eyes were treated with repeated intravitreal injection of ranibizumab (Lucentis; Figure 1A, 1D, 1F, 1G), systemic prednisolone (Figure 1B), and systemic acetazolamide plus local nepafenac (Figure 1E), respectively. The CME shown in Figure 1C resolved spontaneously after resolution of the adhesions of the partially detached posterior hyaloid from the para- and perifovea. It could be that it was caused by vitreomacular traction; hyaloidal traction may stimulate the production of inflammatory factors which is a main cause of CME^[24]. All eyes presented a large cyst in the foveola between the inner

Müller cell layer and the HFL/outer nuclear layer (ONL). The hydrostatic pressure within the cyst caused a detachment of the inner Müller cell layer from the HFL/ONL which was associated with an anterior stretching and elongation of the stalk of the Müller cell cone. The roof of the cyst had a spherical (Figure 1A, 1E) or bispherical shape (Figure 1B-1D, 1G).

In different eyes (Figure 1B, 1D-1G), the detachment of the inner Müller cell layer of the foveola was combined with an elevation of the inner layers of the foveal walls, the presence of smaller cysts in the INL and a schisis between the OPL and HFL of the foveal walls. The schisis was traversed by obliquely arranged bundles of Henle fibers. It is likely that these fiber bundles and the stretched stalk of the Müller cell cone transmitted anterior traction from the elevated inner layers to the central outer foveal layers [as indicated by the more inclined course of the ELM and ellipsoid zone (EZ) lines] which caused abnormalities of the central photoreceptor layer [visible at the irregular reflection intensities of the EZ and interdigitation zone (IZ) lines] or even a detachment of the outer fovea from the RPE. After resolution of CME, the foveal morphology regenerated completely with the exception of remaining irregular reflections of the photoreceptor layer lines which indicates that the regeneration of photoreceptors needs longer time. The mean BCVA of the eyes shown in Figure 1A-1G increased significantly ($P<0.05$) from 0.62±0.21 to 0.88±0.10 from the first visit until the end of the examination periods.

Figure 1H, 1I show SD-OCT images recorded in two eyes of a 52-year-old woman and a 41-year-old man which suffered from uveitis and BRVO, respectively. The patients were treated with systemic prednisolone (Figure 1H) and intravitreal bevacizumab (Avastin; Figure 1I), respectively. The foveas in both eyes showed different patterns of edematous cyst distribution. In the example of Figure 1H, the tractional CME was characterized by large cysts in the INL which caused an anterior displacement of the inner layers [NFL to inner plexiform layer (IPL)] of the foveal walls and parafovea. There was only a small cyst in the foveola. The central ONL was anteriorly stretched and thickened; the anterior displacement of the foveola and foveal walls caused a detachment of the outer fovea from the RPE. The CME shown in Figure 1I was characterized by a large cyst in the foveola and cystic cavities in the INL and between the OPL and HFL of the foveal wall at the right side. The cyst in the foveola caused a detachment of the inner Müller cell layer from the HFL/ONL which was associated with stretching and elongation of the stalk of the Müller cell cone. The central outer retina was little deteriorated, as indicated by the irregular reflection intensities of the EZ and IZ lines. The presence of hyperreflective exudates in the INL

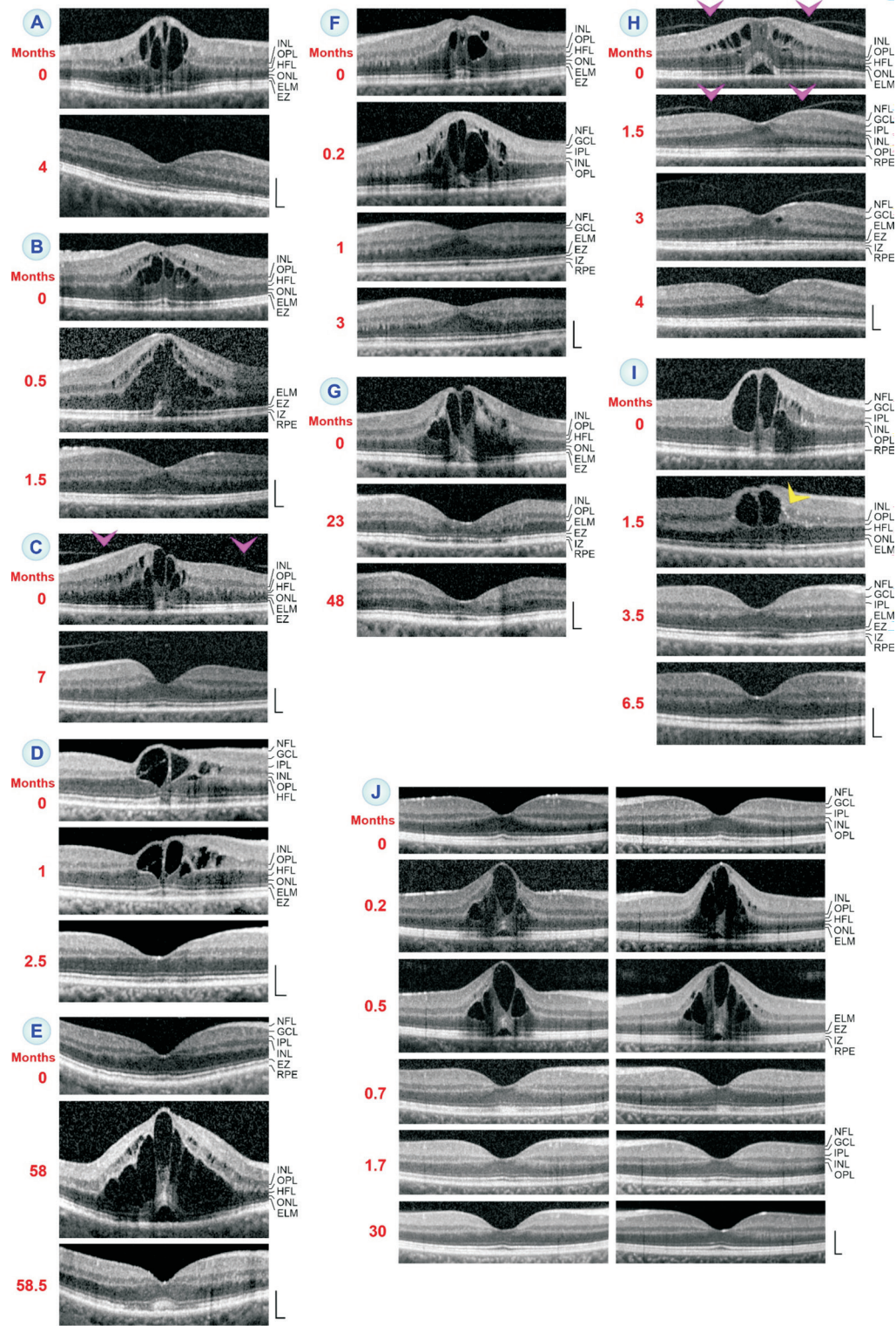


Figure 1 Regeneration of the foveal morphology after resolution of cystoid macular edema (CME) The images show SD-OCT scans through the fovea and parafovea of 11 eyes of 10 patients. The months after the first visit (0) are indicated left of the images. A-G: Morphological regeneration of the fovea after resolution of CME in eyes of different patients. Arrowheads indicate adhesions of the partially detached posterior hyaloid at the para- and perifovea, respectively. H, I: Two eyes with CME with different patterns of edematous cyst distribution, characterized by the absence (H) and presence (I) of a large cyst in the foveola. H: The CME was likely induced by traction of the partially detached posterior hyaloid which adhered at the parafovea (arrowheads). I: Note that the stalk of the Müller cell cone is stretched and elongated. The arrowhead points to hyperreflective dots which represent light reflections at exudates in the inner nuclear layer (INL). J: Simultaneous CME in the foveas of the left (left side) and right eyes (right side) of a patient with uveitis which was treated with systemic prednisolone pulse therapy. The CME resolved rapidly during the subsequent systemic immunosuppressive therapy. Scale bars, 200 μ m. ELM: External limiting membrane; EZ: Ellipsoid zone; GCL: Ganglion cell layer; HFL: Henle fiber layer; IPL: Inner plexiform layer; IZ: Interdigitation zone; NFL: Nerve fiber layer; ONL: Outer nuclear layer; OPL: Outer plexiform layer; RPE: Retinal pigment epithelium.

of the foveal wall at the right side after resolution of the cysts (1.5mo) suggests that the cysts were caused by leaking vessels surrounding the foveal avascular zone. During the examination periods, BCVA increased from 0.5 to 0.8 (Figure 1H) and from 0.6 to 1.0 (Figure 1I), respectively.

Figure 1J shows the simultaneous development and resolution of CME in the foveas of both eyes of a 13-year-old man who suffered from uveitis anterior which was treated with systemic immunosuppressive methotrexate (20 µg once per week). Two days after the first visit, a systemic prednisolone pulse therapy (1 g per 3d) was carried out which resulted in the development of CME. The CME resolved during the subsequent systemic application of methotrexate (25 µg once per week). The CME was characterized by a large central cyst resulting in a detachment of the inner Müller cell layer from the HFL/ONL in the foveola and a high elevation of the inner layers (NFL to OPL) of the foveal walls; the latter resulted in a schisis between the OPL and HFL of the foveal walls, and small cysts in the INL. The inner layers of the foveal walls were kept together centrally by the inner Müller cell layer of the foveola. The anterior traction exerted by the stretched Henle fiber bundles onto the outer foveal layers produced a detachment of the central fovea from the RPE associated with irregular reflection intensities of the ELM and EZ lines, and a central defect of the IZ line. After the rapid resolution of the cystic cavities, the foveal morphology regenerated rapidly and remained stable thereafter. BCVA of both eyes changed from 1.25 (first visit) to 0.80 and 0.50, respectively (0.5mo), and then to 1.00 (0.7 and 30mo).

Foveal Regeneration After Multiple Episodes of Cystoid Macular Edema Complete regeneration of the foveal morphology was also observed in eyes with multiple episodes of CME. Figure 2A shows SD-OCT scans recorded in an eye of a 73-year-old man with development and resolution of an edematous cyst in the foveola during two consecutive times. The eye suffered from BRVO and was treated with intravitreal ranibizumab (Lucentis). The scan recorded at the first visit shows vitreofoveal adhesion and an area in the foveola which was photoreceptor-free, as indicated by the EZ and IZ line defects. The ELM in the photoreceptor-free area displayed an increased reflectivity. After detachment of the posterior hyaloid from the fovea, an edematous cyst developed in the foveola. The hydrostatic pressure within the cyst caused a dehiscence of the ONL in the foveola; the central outer fovea kept together by a glial tissue membrane at the ELM (red arrowhead in Figure 2A). After resolution of the cyst, the dehiscence of the ONL disappeared and the foveal center regenerated, likely by a centripetal displacement of the photoreceptor cells in the ONL and at the ELM, as previously described^[25]. BCVA improved from 0.8 to 1.0 during the examination period.

Figure 2B-2D shows further examples for a twofold development and resolution of CME which were recorded in 3 eyes of 3 patients (2 women, 1 man; mean age, 39.0±16.5y; range 20-49y). The eyes suffered from central retinal vein occlusion (Figure 2B) and uveitis (Figure 2C, 2D), and were treated with intravitreal ranibizumab (Lucentis) injections (6 and 7mo) and panretinal laser coagulation (1.5mo; Figure 2B), systemic prednisolone and intravitreal triamcinolone injection (4mo; Figure 2C), and an intravitreal dexamethason implant (Ozurdex; one week after the first visit; Figure 2D), respectively. The CME of the eye shown in Figure 2C recorded at the first visit was characterized by a large cyst in the foveola, a drawbridge elevation of the inner layers of the foveal walls and parafovea, cystic cavities in the INL, a schisis between the OPL and HFL of the foveal walls and parafovea, and a detachment of the central outer foveal layers from the RPE. During the next 3.7mo, the extent of the elevation of the inner foveal layers varied considerably; this was associated with varying sizes of the intrafoveal cysts and an attachment and redetachment of the central outer fovea from the RPE. After complete resolution of the cysts between 4.5 and 9.5mo and the nearly complete regeneration of the foveal morphology, smaller cysts in the foveola and the INL of the foveal walls developed (12mo). These cysts resolved until 14mo; at this time, the fovea showed a complete morphological regeneration including the absence of irregular reflection intensities of the hyperreflective lines of the outer retina and the presence of a fovea externa, *i.e.*, the inwardly directed cone which is formed by the elongated photoreceptor segments in the foveola and visible in SD-OCT images at the inclined courses of the ELM and EZ lines^[1]. BCVA increased during the examination periods from 0.5 to 1.0 (Figure 2B) and from 0.5 to 0.8 (Figure 2C), respectively. Figure 2D shows SD-OCT images of an eye with different patterns of edematous cyst distribution during both episodes of CME. At the first visit, the fovea showed a large cyst in the foveola and high elevation of the inner layers of the foveal walls which was associated with the formation of cysts in the INL and a schisis between the OPL and HFL, as well as a tractional detachment of the central outer fovea from the RPE. After regeneration of the foveal morphology and subsequent redevelopment of intrafoveal cysts, the inner layers of the foveal walls were elevated again due to large cysts in the INL and between the OPL and HFL. However, there was no cyst in the foveola; instead, the central ONL was anteriorly stretched and thickened which was associated with a detachment of the outer fovea from the RPE. Thereafter, the normal foveal morphology recovered; however, irregular reflection intensities of the central EZ and IZ lines indicate a remaining deterioration of photoreceptors. BCVA increased from 0.4 to 1.0 during the examination period.

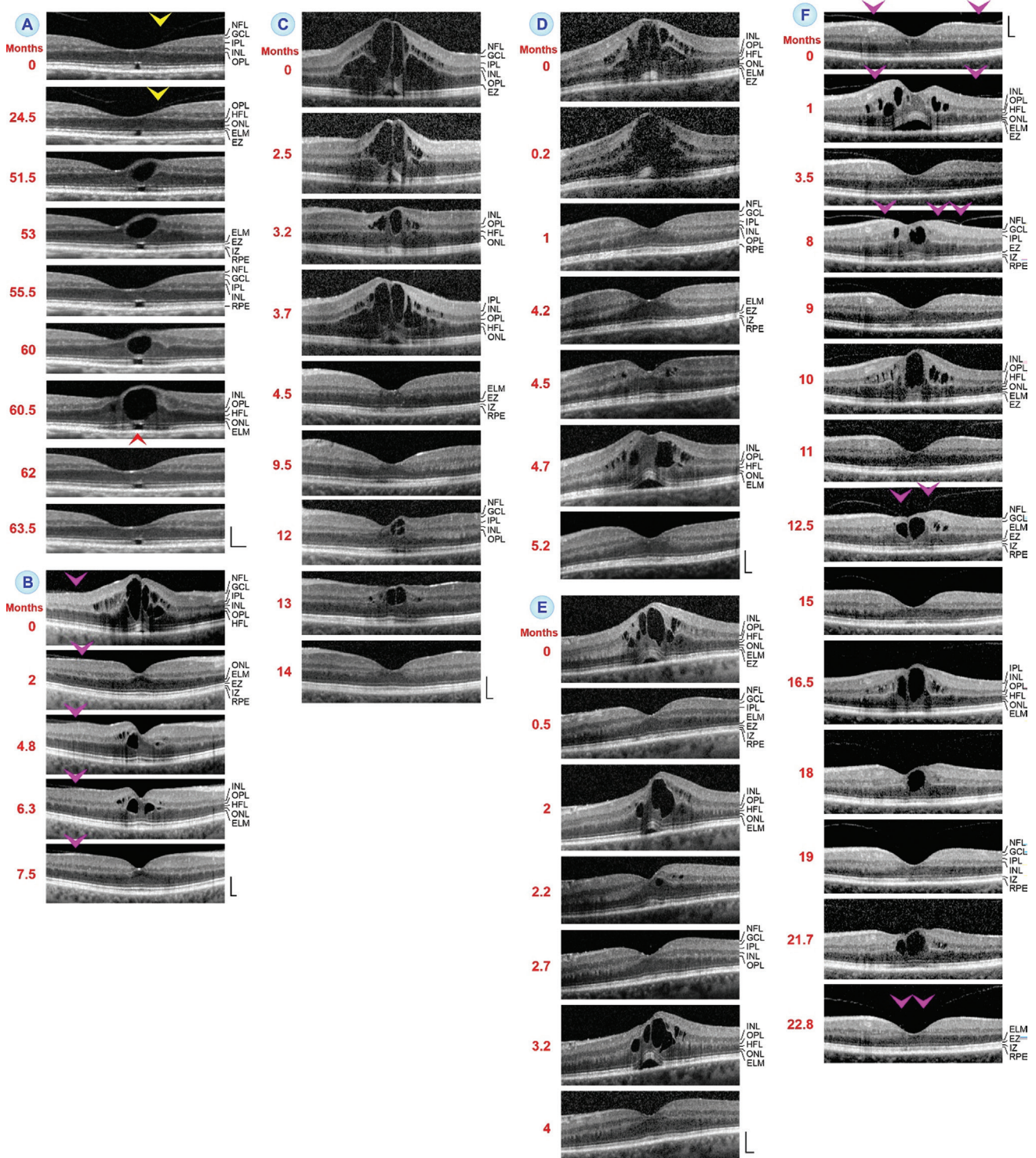


Figure 2 Regeneration of the foveal morphology after twofold (A-D) and multiple episodes (E, F) of cystoid macular edema (CME) The images show SD-OCT scans through the fovea and parafovea of 6 eyes of 6 patients. The months after the first visit (0) are indicated left of the images. A: Twofold development and resolution of an edematous cyst in the foveola. The yellow arrowheads point to adhesion of the partially detached posterior hyaloid. The red arrowhead indicates the glial tissue membrane at the external limiting membrane (ELM) which keeps the central outer fovea together. B: The CME was likely associated with traction of the partially detached posterior hyaloid which adhered at the parafovea (arrowheads). C: Note the irregular reflection intensities of the central ellipsoid zone (EZ) and interdigitation zone (IZ) lines during both episodes of CME which were abrogated at the end of the examination period. D: An eye with different patterns of edematous cyst distribution in both episodes of CME. E: An eye with three CME episodes associated with a detachment of the central outer fovea from the RPE and subsequent regeneration of the foveal morphology. F: An eye with sixfold development of CME. The arrowheads point to foveal adhesions of the partially detached posterior hyaloid. Scale bars, 200 μ m. GCL: Ganglion cell layer; HFL: Henle fiber layer; INL: Inner nuclear layer; IPL: Inner plexiform layer; NFL: Nerve fiber layer; ONL: Outer nuclear layer; OPL: Outer plexiform layer; RPE: Retinal pigment epithelium.

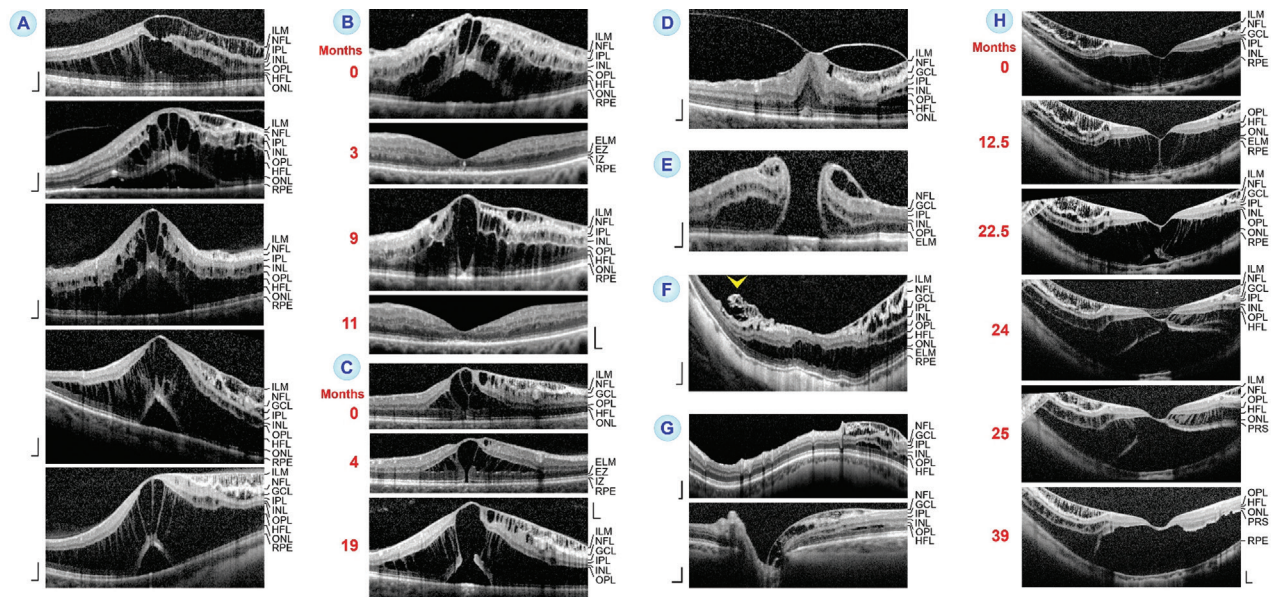


Figure 3 Detachment of the internal limiting membrane (ILM) from the nerve fiber layer (NFL) in different retinal disorders The images show SD-OCT scans through the fovea and parafovea of 12 eyes of 12 patients. The months after the first visit (0) are indicated left of the images. A: Five eyes with cystoid macular edema (CME) and ILM detachment in the tissues at the right side. The images also display a foveoschisis between the outer plexiform layer (OPL) and Henle fiber layer (HFL), cystic cavities in the ganglion cell layer (GCL) and inner nuclear layer (INL), and in four eyes a detachment of the fovea from the retinal pigment epithelium (RPE). In three eyes, the GCL is degenerated. The tissues at the left side of three eyes show no abnormalities with the exception of a large foveoschisis in the HFL. B: An eye with two episodes of CME and ILM detachment. C: Enlargement of an outer lamellar hole (OLH) with ILM detachment and foveoschisis between the OPL and HFL in an eye with CME. D: Fovea of an eye with macular pucker with ILM detachment in the para- and perifovea at the right side. E: An eye with a full-thickness macular hole with ILM detachment in the foveal walls and parafovea. F: An eye with high myopia. The fovea (middle) and wide retinal areas are split by a schisis within the HFL. In addition, there is ILM detachment and schistic cavities in the GCL and INL of the inferior perifovea (right side). In the superior perifovea (left side), the edge of the thickened ILM and parts of the NFL are detached from the remaining NFL (arrowhead). G: An eye with glaucomatous parapapillary retinoschisis in the nasal retina. The image above shows a circumpapillary SD-OCT scan. The image below shows a horizontal SD-OCT scan through the excavated optic disc. H: Development of an OLH with inner and outer retinoschisis in an eye with myopic traction maculopathy. Scale bars, 200 μ m. ELM: External limiting membrane; EZ: Ellipsoid zone; IPL: Inner plexiform layer; IZ: Interdigitation zone; ONL: Outer nuclear layer; PRS: Photoreceptor segments; RPE: Retinal pigment epithelium.

Figure 2E displays SD-OCT scans which were recorded in an eye of a 77-year-old man which suffered from Irvine-Gass syndrome after secondary lens implantation in an aphakic eye; the patient was treated with systemic acetazolamide and ibuprofen plus local nepafenac. The SD-OCT records show three CME episodes associated with a detachment of the central outer fovea from the RPE and subsequent regeneration of the foveal morphology. BCVA was 0.6 and did not increase during the examination period.

Figure 2F shows SD-OCT scans of an eye of a 53-year-old man with diabetic retinopathy which was treated with paracentral laser therapy; the BCVA (0.5) remained stable during the examination period. The SD-OCT records show sixfold development of CME; the foveal morphology regenerated nearly completely between the CME episodes. During the entire examination period, the partially detached posterior hyaloid adhered at the fovea. The first CME episode

(1mo) was characterized by cysts in the INL and between the OPL and HFL of the foveal walls and parafovea; the foveola was anteriorly stretched and thickened, and the fovea was detached from the RPE. The subsequent CME episodes were characterized by the development of a large cyst in the foveola associated with detachment of the inner Müller cell layer from the HFL/ONL, stretching of the stalk of the Müller cell cone, and thinning of the central ONL.

Internal Limiting Membrane Detachment As shown in Figure 3A, CME can also be associated with a detachment of the ILM from the NFL. The scans were obtained from 5 eyes of 5 patients (4 women, 1 man; mean age, 52.2 \pm 24.1y; range 33-85y) which suffered from optic disc pit, Irvine-Gass syndrome, diabetic retinopathy, and chorioretinitis, respectively; the mean BCVA was 0.52 \pm 0.25. ILM detachment led to the formation of a schisis between the thickened ILM and NFL which was vertically traversed by hyperreflective

Müller cell trunks. Figure 3B shows SD-OCT scans recorded in an eye of a 56-year-old woman who suffered from diabetic retinopathy (BCVA, 0.5). The scans show two episodes of CME development. In addition to the cystic spaces in the foveola and the INL and HFL of the foveal walls and parafovea, there was ILM detachment in the foveal wall and parafovea at the right side. CME and ILM detachment were associated with neuronal and photoreceptor degeneration, as indicated by the absence of a regular GCL, a thinning of the foveola, and the absence of a fovea externa after edema resolution.

Figure 3C shows the enlargement of an OLH with ILM detachment and foveoschisis between the OPL and HFL in an eye with CME of a 47-year-old man who suffered from optic disc pit; BCVA fluctuated between 0.32 and 0.50 during the examination period. The OLH was caused by elevation of the inner layers of the foveola and foveal walls; the oblique anterior traction transmitted by the bundles of erected Henle fibers within the foveoschisis caused a disruption of the central outer fovea. The thickness and lateral extension of the foveoschisis between the OPL and HFL was related to the height of the inner layers of the foveal walls. Anterior traction increased the base diameter of the OLH via a detachment of the central outer fovea from the RPE. The schisis between the ILM and NFL and the cystic cavities in the INL of the parafovea resolved transiently (4mo) and developed again (19mo).

In addition to eyes with CME, ILM detachment was also found in eyes with other kinds of foveal and retinal defects. Figure 3D shows a fovea of a 59-year-old woman with macular pucker with ILM detachment in the para- and perifovea (BCVA, 0.4). Anterior vitreofoveal traction exerted by the partially detached posterior hyaloid, which adhered at the peripheral margin of the Müller cell cone, caused stretching and thickening of the foveola. The para- and perifovea at the right side shows a schisis between the detached ILM and NFL, cystic cavities in the GCL and INL, and a schisis in the HFL. Figure 3E shows an FTMH with ILM detachment in the foveal walls and parafovea in an eye of a 73 year-old man (BCVA, 0.5). In the tissue at the right side, most stretched Müller cell trunks between the detached ILM and NFL were disrupted.

Figure 3F shows the macula of a highly myopic eye of a 47 year-old woman (BCVA, 0.1). There were outer and inner retinoschisis; the large outer retinoschisis within the HFL was vertically traversed by bundles of Henle fibers. The inner retinoschisis resulted from ILM detachment and schistic cavities in the GCL and INL; the schistic cavities were vertically traversed by bundles of Müller and neuronal cell fibers. In the superior perifovea, the edge of the thickened ILM and parts of the NFL, including the Müller cell trunks between

both, were detached from the remaining NFL (arrowhead in Figure 3F). Figure 3G displays SD-OCT scans obtained from a 72-year-old man with glaucomatous parapapillary retinoschisis in the nasal retina (BCVA, 1.0). In addition to the ILM detachment, there was schistic splitting of the GCL, INL, and HFL; the schistic cavities were vertically traversed by hyperreflective trunks and linked to the optic disc pit.

Figure 3H shows the development of an OLH with inner and outer retinoschisis in an eye with myopic traction maculopathy of a 42-year-old man. The large outer retinoschisis in the HFL was nearly vertically traversed by bundles of Henle fibers. In addition, there was ILM detachment and schistic splitting of the GCL and INL. The inner Müller cell layer of the foveola kept the inner layers (NFL to OPL) of the foveal walls together, and the vertical stalk of the Müller cell cone was strongly stretched; this caused a detachment of the central outer retina from the RPE (22.5mo). Thereafter, the stalk of the Müller cell cone disrupted; this was associated with a disruption of the central outer fovea, *i.e.*, the establishment of the OLH. Subsequently, the area of retinal detachment from the RPE increased; this was associated with a complete resolution of the ILM detachment and the schistic cavities in the INL and HFL. BCVA decreased from 0.6 to 0.2 during the examination period.

Internal Limiting Membrane Detachment in Eyes with Fundus Light Reflections Figure 4A-4C shows fundus and SD-OCT records of three unrelated women with MCSD (mean age, 62.0 ± 7.2 y; range 56-70y). Light reflections at the retinal surface often followed the folds of the retinal surface and were also present along the large superficial vessels; in various areas, the reflections were arranged as stellate rays oriented towards the fovea (Figure 4Aa, 4Ca). In the circumpapillary SD-OCT scan of the left eye (BCVA, 0.2) of a patient with late-stage MCSD (Figure 4Ab above), the ILM and NFL were hyperreflective; the hyporeflectivity of the GCL indicates a degeneration of retinal ganglion cells. In the right eye (BCVA, 0.2; Figure 4Ab middle and below), the disease was more advanced. ILM detachment at many sites resulted in folding of the retinal surface. There was a large schisis within the INL. Vertical hyperreflective trunks, likely composed of Müller cells, traversed the tissue from the ILM to the OPL. The OPL had an undulating appearance; the crests of the OPL waves were connected to the vertical hyperreflective trunks. This may suggest that the OPL waves were created by tractional forces which originated in the folds of the detached ILM and transmitted by the vertical trunks of Müller cells. The horizontal scan through the fovea of the left eye (Figure 4Ac) shows a CME with a large cyst in the foveola and a drawbridge elevation of the inner layers (NFL to OPL) of the foveal walls combined with a schisis within the HFL. The ONL below

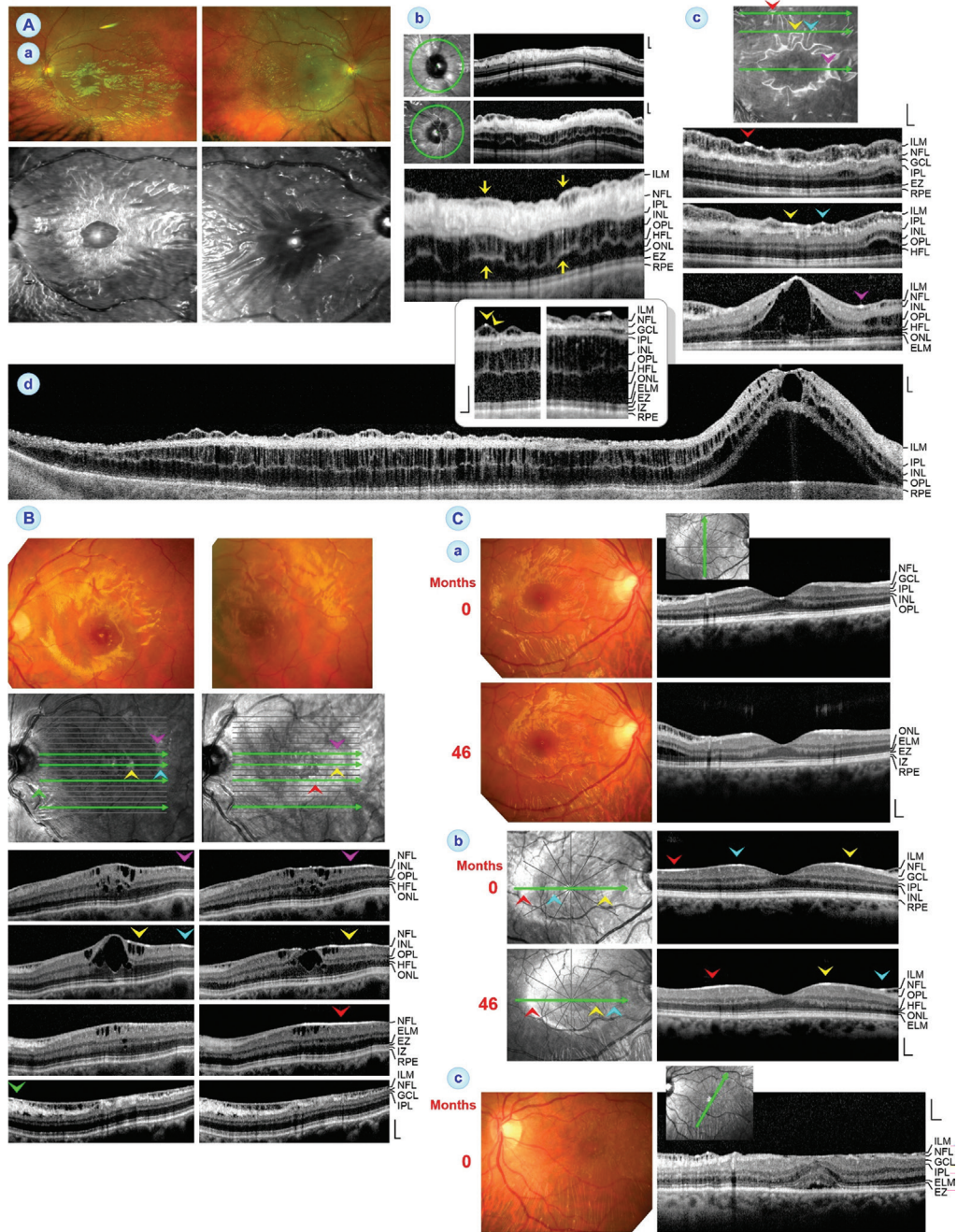


Figure 4 Müller cell sheen dystrophy (MCSD) is associated with cystoid macular edema (A, B) and internal limiting membrane (ILM) detachment (A-C). The images show fundus images and SD-OCT scans through the fovea and parafovea of 5 eyes of 3 patients. The arrowheads with different colors in A, B, and C indicate corresponding light reflections in the fundus images and SD-OCT scans, suggesting that the light was reflected at the detached ILM and nerve fiber layer (NFL; left side in Cb). **A:** Fundus images (a) of the left (left side) and right eye (right side), and SD-OCT records (b-d) of a patient with late-stage MCSD. The images shown in c and d were recorded three weeks after recording of the images shown in a and b. a: The macular region of the right eye appears dark because of massive subretinal fluid. b: Circumpapillary SD-OCT scans of the left (above) and right eye (middle and below). The yellow arrows indicate vertical hyperreflective trunks which traverse the tissue from the detached ILM to the outer plexiform layer (OPL). c: Horizontal SD-OCT scans through the foveal center and the retina at two different distances from the fovea in the left eye. d: Composite SD-OCT image of the fovea (right side) and more peripheral retinal areas (left side) of the right eye. There was cystoid edema in the foveal tissue and a serous detachment of the fovea from the retinal pigment epithelium (RPE). The inset shows the mid-peripheral retina at two sites at higher magnification. The arrowheads indicate two hyperreflective trunks which spanned vertically between the detached ILM and the OPL. Note the light reflection at the crest of the ILM fold. **B:** Fundus images (above) and SD-OCT scans (below) of an eye with MCSD of another patient. The images were recorded at the first visit (left) and 1.5mo later (right). **C:** Fundus and SD-OCT images recorded in the right (a, b) and left eye (c) of a further patient with MCSD. The images in a and b were recorded at the first visit (0mo) and 46mo later. Scale bars, 200 μ m. ELM: External limiting membrane; EZ: Ellipsoid zone; GCL: Ganglion cell layer; HFL: Henle fiber layer; INL: Inner nuclear layer; IPL: Inner plexiform layer; IZ: Interdigitation zone; ONL: Outer nuclear layer.

the large central cyst had a decreased thickness. There was large ILM detachment in the parafovea and more peripheral retinal areas as well as schistic cavities in the GCL and INL, and between the OPL and ONL. The detached ILM had an undulating appearance which caused the folds of the inner retinal surface. Figure 4Ad shows a composite SD-OCT image of the retina of the right eye. The fovea displayed a CME and was detached from the RPE. The more peripheral retina was thickened and contained large cysts in the INL and HFL; the cysts in both layers were separated by horizontal structures of the OPL and vertically traversed by hyperreflective trunks. In addition, there were areas with ILM detachment.

Figure 4B shows fundus and SD-OCT images of an eye with MCSD of another patient (BCVA, 0.6). The absence of retinal surface folds may suggest that it is an early stage of MCSD. The foveal morphology was disrupted by a large cyst in the foveola which caused a detachment of the inner Müller cell layer of the foveola from the HFL/ONL, a partial dehiscence of the central ONL, and a flattening of the fovea externa associated with irregular reflectivities of the EZ and IZ lines. ILM detachment was present in more peripheral areas; this was associated with a hyporefectivity of the GCL, likely caused by degeneration of retinal ganglion cells. The SD-OCT images of Figure 4Ca and 4Cb, which were recorded in the right eye of one further patient with MCSD (BCVA, 1.0), showed ILM detachment in the nasosuperior retina. In the superior macula, the ILM detachment was associated with the development of a schisis between the OPL and HFL/ONL (Figure 4Ca). The left eye (BCVA, 0.8) showed ILM detachment in the inferior perifovea (Figure 4Cc). The fovea was detached from the RPE likely by elevation and centripetal displacement of the foveal walls due to proliferation of an ERM which lay at the foveal center and that merged with the thickened ILM. Light reflections which followed the folds of the retinal surface were present in the inferior, but not superior fundus, suggesting that the folds were caused by the waves of the detached ILM.

In SD-OCT images of the three subjects with MCSD (Figure 4A-4C), the thickness of the detached ILM ranged from 15 to 27 μm ; this is considerably thicker than the thickness of the basal lamina of the ILM outside of the foveal pit in subjects without eye disease (0.9-4.3 μm)^[7,26]. In the fundus and SD-OCT images of Figure 4Ac, 4B, and 4Cb, corresponding light reflections are marked by arrowheads. The corresponding localizations of the reflections in both types of images show that in eyes with MCSD the light was reflected at the detached (Figure 4Ac, 4B) or nondetached ILM (Figure 4Cb), or the NFL (temporal macula of the examples shown in Figure 4B and 4Cb).

Fundus light reflections can also be found in retinal disorders without ILM detachment like in eyes with cellophane maculopathy or macular pucker. Figure 5A shows fundus and

SD-OCT images obtained in two eyes of two (53 and 64-year-old) women with cellophane maculopathy. The cellophane-type ERM produced macular reflexes in fundus images. There were no folds of the inner retinal surface. In the examples of two eyes of two (59 and 72-year-old) women with macular pucker and fundus light reflections shown in Figure 5B, traction exerted by ERM caused folds and thickening of the inner retinal layers and, in the left example, a macular pseudohole.

DISCUSSION

In CME, the foveola as well as the INL and HFL of the foveal walls and parafovea are the preferred locations of edematous cysts^[8-11]. However, the pattern of edematous cyst distribution may not only vary between different eyes with CME (Figure 1H, 1I) but also in single eyes during different CME episodes (Figure 2D, 2F). There are CME with cystic cavities in the INL and HFL of the foveal walls and parafovea, but not in the foveola; this cyst distribution is associated with anterior stretching and thickening of the foveola, and a detachment of the central fovea from the RPE (Figure 2D, 2F). In other types of CME, there is also a prominent cyst in the foveola; the hydrostatic pressure within the cyst causes a detachment of the inner Müller cell layer of the foveola which is associated with stretching (Figures 1A-1D, 1F, 1G, 1I, 2B-2F, 3B) and/or disruption of the vertical stalk of the Müller cell cone (Figures 1E, 1J, 3B, 3C, and 4Ac, 4B), and a dehiscence of the central ONL (Figures 1D, 2A, 2B, 2F, and 4Ac, 4B). The roof of the cyst in the foveola has a spherical (Figures 1A, 1E, 3A-3C, and 4Ac, 4B) or bispherical shape (Figures 1B-1D, 1G and 3B); the latter is apparently caused by traction of the stretched stalk of the Müller cell cone. Disruption of the stalk of the Müller cell cone may result in dehiscence of the central ONL (Figures 1J and 4Ac, 4B), the loss of the shape of the fovea externa (Figures 3B and 4Ac, 4B), or the formation of an OLH when the ELM becomes simultaneously disrupted (Figure 3C, 3H).

The detachment of the inner Müller cell layer from the HFL/ONL in the foveola is often combined with an elevation of the inner layers of the foveal walls; this may cause the formation of a foveoschisis between the OPL and HFL of the foveal walls which is obliquely traversed by bundles of Henle fibers (Figures 1B, 1C, 1E-1G, 1J, 2B-2E, 3A-3C, and 4Ac). The erection of the Henle fibers indicates that the Müller cells of the foveal walls change their morphology from the z-shape to a straighter shape (Figure 6). The stretched Müller cells transmit the anterior traction from the elevated inner layers to the central outer fovea which may result in abnormalities of the central photoreceptor layer or a detachment of the outer fovea from the RPE (Figures 1B, 1E-1G, 1J, 2B-2E, and 3A, 3B)^[8,27-28]. This detachment results most likely from the facts that the elevation of the inner foveal layers is highest at the central edges of the

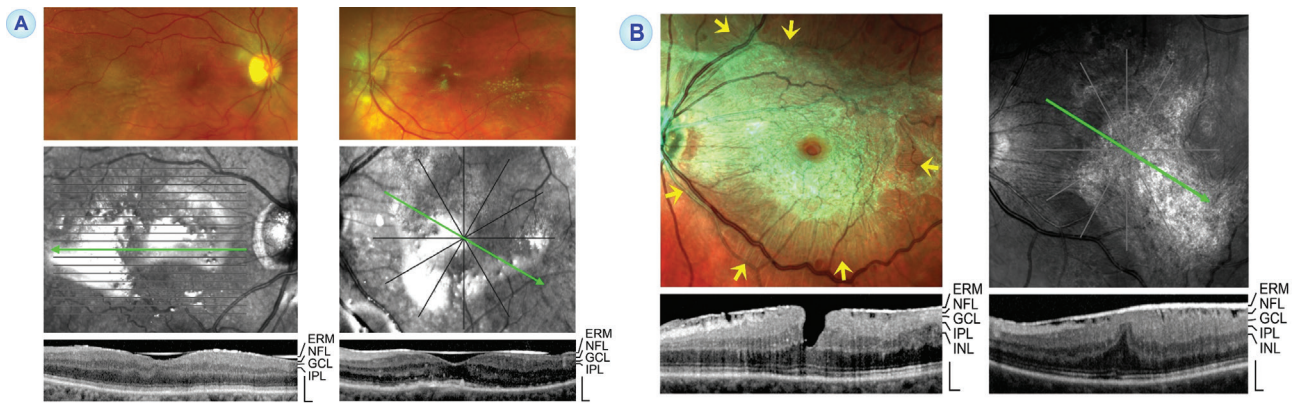


Figure 5 Fundus light reflections in eyes with cellophane maculopathy and macular pucker, respectively. A: Fundus (above) and SD-OCT images (below) of two eyes of two patients (left and right) with cellophane maculopathy. B: Fundus (above) and SD-OCT images (below) of two eyes of two patients (left and right) with macular pucker and fundus reflections. Left: There is also a macular pseudohole. The arrows indicate the directions of the retinal folds in the mid-peripheral retina. Right: Note that the light-reflecting part of the epiretinal membrane (ERM) is thicker than nonreflecting part. Scale bars, 200 µm. GCL: Ganglion cell layer; INL: Inner nuclear layer; IPL: Inner plexiform layer; NFL: Nerve fiber layer.

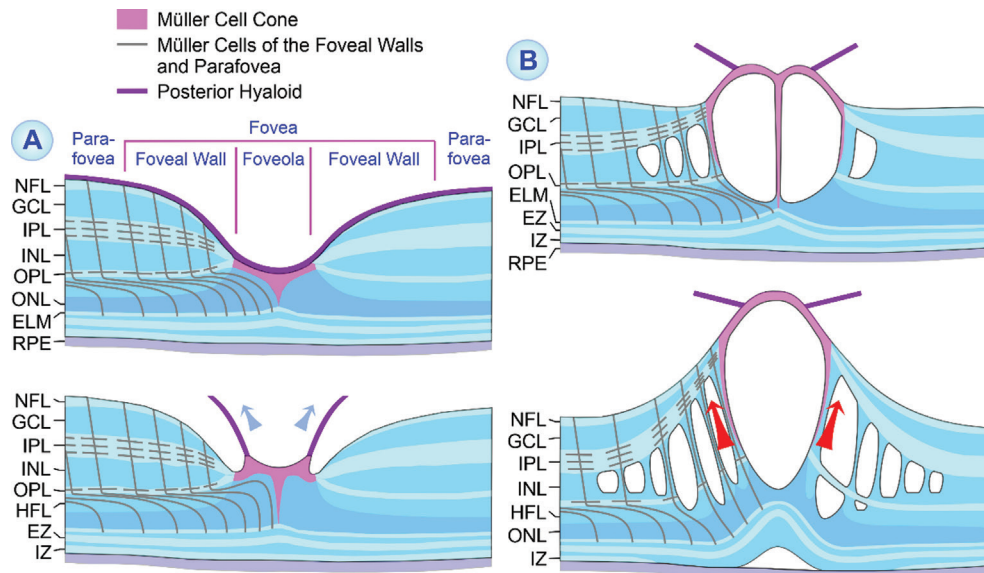


Figure 6 Foveal deformation caused by tractional cystoid macular edema. A: Perifoveal posterior vitreous detachment. The partially detached posterior hyaloid causes anterior traction which stretches the foveal center. B: The development of an edematous cyst in the central fovea results in a detachment of the inner Müller cell layer from the Henle fiber layer (HFL)/outer nuclear layer (ONL) in the foveola. This is associated with an elongation and subsequent disruption of the stalk of the Müller cell cone. Edematous cysts are also present in the inner nuclear layer (INL) of the foveal walls which are spanned by bundles of Müller and bipolar cell fibers. The enlargement of the cysts causes an anterior traction which is transmitted by the stretched and straightened Müller cells of the foveal walls from the inner to the outer foveal layers. This may cause abnormalities of the central photoreceptor layer and (when the elevation of the inner layers of the foveal walls exceeds the length of Müller cells and their capacity for cell stretching) a detachment of the fovea from the retinal pigment epithelium (RPE). Fluid accumulation in the subretinal space may impair the fluid clearance from the outer foveal layers through the RPE, resulting in the formation of edematous cysts in the HFL. ELM: External limiting membrane; EZ: Ellipsoid zone; GCL: Ganglion cell layer; IPL: Inner plexiform layer; IZ: Interdigitation zone; NFL: Nerve fiber layer; OPL: Outer plexiform layer.

foveal walls and that the centralmost Müller cells of the foveal walls are shortest; therefore, the anterior traction exerted by the cells onto the outer retina is strongest in the center of the foveola (Figure 6)^[29]. Mathematical modeling revealed that the stiffness of Müller cells of the foveal walls and parafovea in myopic traction maculopathy (Figure 3H) increases with the

anterior stretching and straightening of the cells; the greater rigidity increases the capacity of Müller cells to transmit tractional forces from the inner to the outer retina^[28]. The locations of the cysts in the foveola and the foveoschisis in the foveal walls and parafovea can be explained with the location of the tissue layer interfaces with the lowest mechanical

cohesion: the boundary between the Müller cell cone and the HFL/ONL in the foveola, and the interface between the OPL and HFL in the foveal walls and parafovea^[30]. The absence of cellular connections between the cells, which form the Müller cell cone, and the outer processes of Müller cells of the foveal walls, which surround the photoreceptor cells in the HFL and ONL^[7], facilitates the detachment of the inner Müller cell layer from the HFL/ONL in the foveola if excess fluid accumulates within this tissue border.

CME with cysts predominantly in the INL, but not in the HFL (Figures 1H and 2F), is probably caused by vascular leakage (Figure 1I) and/or impaired fluid clearance from the inner retina due to traction-induced dysfunction of Müller cells of the foveal walls and parafovea^[10]. Fluid which enters the retinal parenchyme from leaky vessels of the intermediate and deep vascular plexus accumulates within the INL because the IPL and OPL are diffusion barriers which limit intraretinal fluid distribution^[9]. The formation of edematous cysts in the foveola, with the roof formed by the detached inner Müller cell layer, may suggest that the inner layer of the foveola also represents a high-resistance barrier for paracellular fluid movement; this layer is formed by a plait of multiple stacks of thin sheaths of Müller cell processes^[7]. Fluid which enters the retinal parenchyme from leaky vessels of the superficial vascular plexus is normally drained into the vitreous cavity; therefore, edematous cysts are usually not formed in the GCL (Figures 1B-1I, 1J, and 2B-2F)^[10]. However, in eyes with thickened and tightened ILM caused by hypertrophied and proliferating astrocytes which produce new collagen^[13,31], the ILM may become a barrier against fluid clearance. Therefore, fluid leaking from superficial vessels cannot be drained into the vitreous cavity resulting in the formation of edematous cysts in the GCL and/or a schisis between the ILM and NFL, *i.e.*, ILM detachment (Figures 3A-3C and 4B). Cystic or schistic cavities in the HFL may be caused by edema formation (*i.e.*, leakage of the vessels of the deep vascular plexus and/or impaired fluid clearance due to detachment of the outer retina from the RPE or dysfunction of RPE cells) or may represent tractionally induced pseudocysts resulting from the elevation of the inner layers of the foveal walls and parafovea (foveoschisis)^[32].

Two to 10% of highly myopic eyes investigated in different studies showed tractional ILM detachment^[15,17,19]. In these eyes, ILM detachment was often seen in the periphery (Figure 3F, 3H); the detachment may reach the parafovea starting from the peripheral locations^[17]. ILM detachment is also often found in eyes with optic disc pit and peripapillary retinoschisis (Figure 3G)^[20]. We show that (in addition to eyes with CME, myopic traction maculopathy or parapapillary retinoschisis) ILM detachment may also occur in eyes with macular pucker (Figure 3D), FTMH (Figure 3E), OLH (Figure 3C), and

MCS (Figure 4A-4C). Detached ILM is thickened and has an increased rigidity, likely resulting from gliosis of fibrous astrocytes; astrocytes in the NFL hypertrophy, proliferate, migrate to the basal lamina at the inner retinal surface, are coupled *via* gap junctions, and produce new collagen^[13,31,33]. Rigid ILM may exert vitread traction which causes the schisis between the detached ILM and NFL^[8,15]. ILM detachment is possible because the Müller cell endfeet are laterally connected at their vitreal edges; the schisis develops within the layer of the Müller cell endfeet which lies between the ILM and NFL. Thus, the vertical Müller cell trunks between the detached ILM and NFL likely represent stretched and thickened Müller cell endfeet. As found in the eye with FTMH (Figure 3E), longstanding ILM detachment may result in disruption of the stretched Müller cell endfeet^[19]. We show one example of a detachment of the thickened ILM and a part of the NFL, including the Müller cell trunks between both, from the remaining NFL (Figure 3F). This kind of detachment is likely caused by increased stiffness of the thickened ILM, which causes anterior traction, and shows that the stretched Müller cell endfeet which traverse the schisis also have an increased stiffness. The increased stiffness may be caused by upregulation of glial intermediate filaments like GFAP; GFAP is usually not expressed by Müller cell endfeet^[11]. Upregulation of intermediate filaments is a common response of Müller cells to retinal injury and disease^[34] and increases the stiffness of the cells^[35]. The colocalization of detached ILM and OPL waves (Figure 4Ab, 4Ad) and the schisis between the OPL and HFL/ONL (Figure 4Ca), respectively, may indicate that the anterior traction exerted by the detached ILM is transmitted by Müller cells from the inner to the outer retina, and may be implicated in the formation of outer retinoschisis.

In eyes with MCS, CME is assumed to be caused by diffuse retinal capillary permeability which is associated with endothelial cell swelling, pericyte degeneration, and basement membrane thickening^[21-23]. It was suggested that cystic cavities in eyes with MCS initially develop between the ILM and NFL of the periphery and peripheral retina; thereafter, the cystic degeneration spreads towards the fovea and outer retinal layers during several years between the fifth and eighth decade of life^[22]. In eyes with early-stage MCS characterized by the absence of significant cell loss, we observed that ILM detachment was present in mid-peripheral, but not in central retinal areas (Figure 4B, 4C); however, the nondetached ILM or NFL in the para- and periphery were thickened and/or tightened in two eyes which was associated with fundus light reflections (Figure 4B, 4Ca). When CME develops in the fovea (Figure 4Ac, 4Ad, 4B), visual acuity declines^[22-23]. Electroretinography revealed a selective reduction of the b-wave amplitude which may reflect a dysfunction of Müller

cells^[21]. The time-dependent progression of the edematous alterations from the inner to the outer retina may be caused by the progression of vascular leakage and gliotic alterations of Müller cells. We found in the eye with late-stage MCS D that the GCL and INL were largely atrophic whereas remnants of the ONL were present (Figure 4Ad). It could be that photoreceptor cells in the ONL of eyes with late-stage MCS D may survive because they are nourished by choroidal vessels and not by the retinal vasculature. The cysts in the INL and ONL were separated by horizontal structures of the OPL, likely formed by laterally connected side processes of Müller cells^[1], and vertically traversed by hyperreflective trunks, likely formed by the main processes of Müller cells.

We found that fundus light reflections can be caused by different highly reflective membranes or layers at the retinal surface: the thickened and tightened ILM (Figure 4Ac, 4B, 4Cb), the NFL which is likely tightened by gliosis of astrocytes (temporal macula of the examples shown in Figure 4B and 4Cb), or idiopathic ERM; the latter may represent simple noncontractile ERM as in cellophane maculopathy (Figure 5A) or contractile ERM (Figure 5B). Fundus light reflections caused by thickened and tightened ILM can be found in retinal areas without (nasal para- and perifovea of Figure 4Cc) and with ILM detachment (Figure 4Ac). All these structures are partly formed by activated and gliotic astrocytes. It was shown that cellophane-like ERM contain collagen types different to those found in tractional ERM^[36]. It could be that the type of collagen produced by activated astrocytes determines whether membranes or layers at the retinal surface causes strong light reflection. The spatial distribution of the light reflections in fundus images of eyes with ILM detachment is also dependent on the distribution of the ILM folds. The predominant astrocytic composition of ERM and thickened ILM may also explain the association between the ERM and ILM found in one eye (Figure 4Cc).

Most eyes with transient CME presented in this study showed a complete or nearly complete regeneration of the foveal morphology after resolution of edema (Figures 1A-1J and 2A-2F). Fast transient CME may cause a disruption of the photoreceptor segments whereas photoreceptor cell somata in the ONL survive and regenerate receptor segments after resolution of edema which preserves visual acuity. Chronic edema, however, is a major cause of tissue degeneration and severe impairment of vision resulting from damage to photoreceptors and neurons^[37]. We present one eye with multiple episodes of transient CME which were associated with a degeneration of photoreceptor cells and inner foveal neurons (Figure 3B). Whether degeneration of photoreceptor cells and/or defects of the photoreceptor layer remain after edema resolution is likely dependent on various factors, including

the duration of the detachment of the outer fovea from the RPE. In eyes with short single or multiple CME episodes, the central fovea regenerated either completely, which includes the disappearance of irregularities of the photoreceptor layer lines and the reformation of a regular fovea externa (Figures 1F, 1J and 2B, 2C), or nearly completely with remaining irregularities of the central photoreceptor layer lines (Figures 1C-1E, 1G-1I and 2D-2F).

The examples of a complete regeneration of the foveal morphology after transient CME (Figures 1A-1J and 2A-2F) show that the fovea may withstand even large tractional deformations and has a conspicuous capacity of structural regeneration after a cystic disruption of the tissue as long as no cell degeneration occurs. We suggest that the regenerative capacity depends on the integrity of Müller cells which form, together with retinal astrocytes in the para- and perifovea, the structural framework of the fovea. In disorders associated with cell degeneration, the glial cell network may maintain the retinal structure even after loss of most retinal neurons as in the late stage of MCS D (Figure 4Ad).

The disruption of the foveal morphology caused by CME allows the identification of the glial scaffold which stabilizes the foveal structure. A schematic representation of this glial cell network is shown in Figure 7. The horizontal stability is provided by the inner horizontal layer of the Müller cell cone in the foveola, the side processes of the Müller cells in the INL and OPL of the foveal walls and parafovea, the laterally connected Müller cell endfeet at the ILM, the astrocytic network in the NFL, and the ELM. The vertical stability is provided by the vertical stalk of the Müller cell cone in the foveola and the main processes of the Müller cells of the foveal walls and parafovea; the latter maintain the rows of stacked neuronal cell somata in the inner foveal layers and the curved rows of the photoreceptor cell somata in the ONL. The Müller cell cone provides the stability for the central fovea. The horizontal layer of the Müller cell cone is laterally connected to the NFL, IPL, and OPL of the foveal walls and keeps the inner layers of the walls (NFL to OPL) together (Figure 7). Therefore, edematous or tractional detachment of the inner Müller cell layer from the HFL/ONL in the foveola may be associated with a drawbridge elevation of the inner layers of the foveal walls and a schistic splitting of the walls between the OPL and HFL (Figures 1B, 1E, 1G, 1J and 2C, 2E). The occurrence of ILM detachments suggests that the horizontal glial structure at the NFL is formed by two components: the three-dimensional network of astrocytes in the NFL and the vitreous-facing membranes of the Müller cell endfeet which are laterally connected.

It was shown that deformation of Müller cells results in cell stretching and subsequent relaxation which can be described

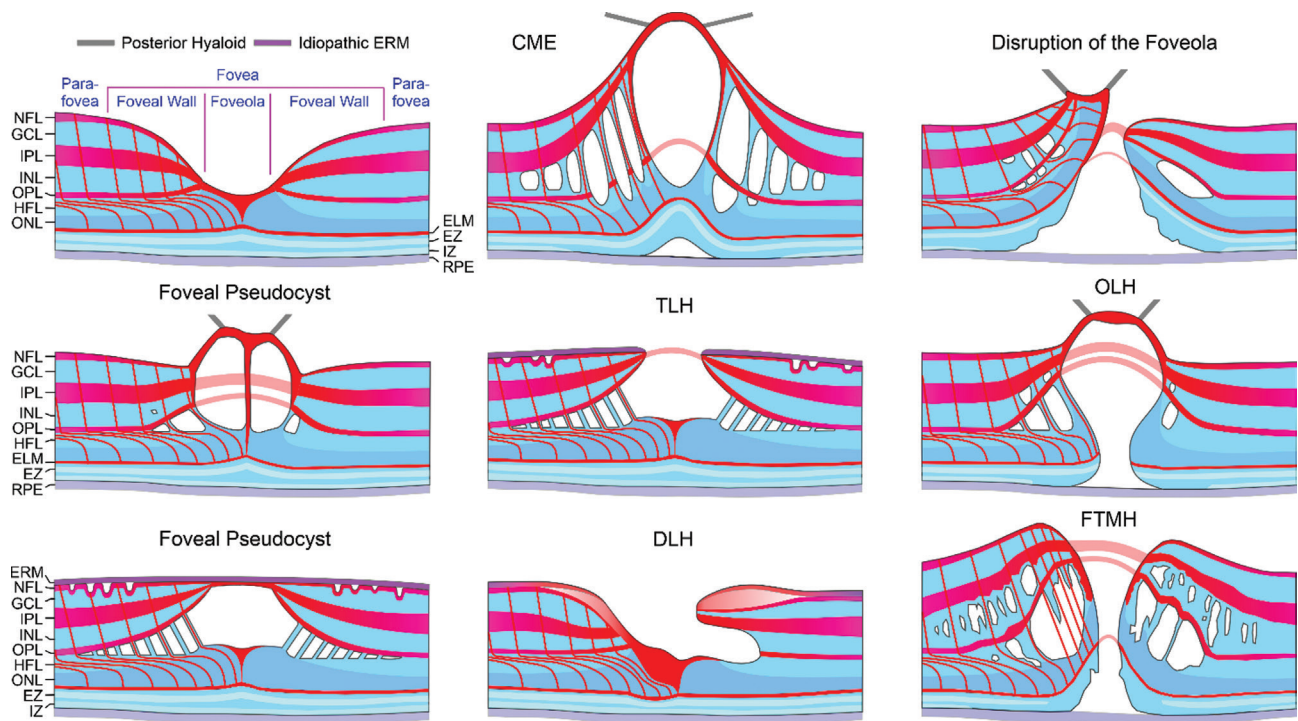


Figure 7 Schematic representation of the glial cell network (red) which provides the mechanical stability of the normal fovea (left above) and of foveas with various kinds of tractional disorders In foveal pseudocysts generated by anterior hyaloidal traction (left middle), the horizontal layer of the Müller cell cone is detached from the Henle fiber layer (HFL)/outer nuclear layer (ONL) in the foveola. In foveal pseudocysts generated by contractile idiopathic epiretinal membranes (ERM; left below), traction of ERM causes a drawbridge elevation of the inner layers [nerve fiber layer (NFL) to outer plexiform layer (OPL)] of the foveal walls and a foveoschisis between the OPL and HFL. A foveoschisis can also be found in tractional lamellar holes (TLH) and outer lamellar holes (OLH). In TLH, degenerative lamellar holes (DLH), and full-thickness macular holes (FTMH), the horizontal layer of the Müller cell cone in the foveola is disrupted. In OLH and FTMH, the external limiting membrane (ELM) is disrupted; this is also the case after a tractional disruption of the entire foveola. In cystoid macular edema (CME), foveal pseudocysts, and OLH, the vertical stalk of the Müller cell cone in the foveola may be disrupted while the horizontal layer of the Müller cell cone keeps the inner layers of the foveal walls together. GCL: Ganglion cell layer; EZ: Ellipsoid zone; INL: Inner nuclear layer; IPL: Inner plexiform layer; IZ: Interdigitation zone; RPE: Retinal pigment epithelium.

as a behavior similar to a restoring spring (elastic part) and a dissipative dashpot (viscous part); the resulting overdamped viscoelastic behavior of the cells is comparable to shock absorbers^[38]. Thus, Müller cells may protect neurons from mechanical injury caused, for example, by orbital trauma or movements of the shrunken vitreous body in the aged eye^[38]. We hypothesize that the threedimensional glial scaffold of the fovea, which is composed of Müller cell and astrocyte processes, functions as a viscoelastic network which mediates the regeneration of the foveal morphology after resolution of CME or traction to the fovea. The structural stabilization of the tissue by glial cells is supported by intermediate filaments like GFAP^[3]. A high expression level of GFAP is found in the inner Müller cell layer of the foveola and the OPL of the foveal walls and parafovea, as well as in astrocytes^[1,39]. The GFAP-expressing inner layer of the Müller cell cone is connected to the GFAP-expressing Müller cell processes in the OPL^[39]; both lie just above the tissue layer interfaces with the lowest mechanical coherence^[30]. Thus, the inner Müller cell layer of

the foveola and the side processes of Müller cells in the OPL are suggested to provide the main horizontal stability of the fovea. In eyes with disruption of parts of the glial scaffold, *e.g.*, the Müller cell cone in inner lamellar holes, ELM in OLH, or both in FTMH, traction exerted by the scaffold may contribute to further alterations of the foveal morphology.

ACKNOWLEDGEMENTS

Authors' contributions: Bringmann A, Kohen L, and Wiedemann P designed the experiments. Karol M, Unterlauff JD, Barth T, Wiedemann R, and Rehak M performed the experiments. Bringmann A performed the data analysis and wrote the paper. Kohen L and Wiedemann P revised the paper. All authors read and approved the final manuscript.

Conflicts of Interest: **Bringmann A**, None; **Karol M**, None; **Unterlauff JD**, None; **Barth T**, None; **Wiedemann R**, None; **Kohen L**, None; **Rehak M**, None; **Wiedemann P**, None.

REFERENCES

- 1 Bringmann A, Syrbe S, Görner K, Kacza J, Francke M, Wiedemann P, Reichenbach A. The primate fovea: structure, function and

- development. *Prog Retin Eye Res* 2018;66:49-84.
- 2 MacDonald RB, Randlett O, Oswald J, Yoshimatsu T, Franze K, Harris WA. Müller glia provide essential tensile strength to the developing retina. *J Cell Biol* 2015;210(7):1075-1083.
 - 3 Reichenbach A, Hagen E, Schippel K, Eberhardt W. Quantitative electron microscopy of rabbit Müller (glial) cells in dependence on retinal topography. *Z Mikrosk Anat Forsch* 1988;102(5):721-755.
 - 4 Holländer H, Makarov F, Dreher Z, van Driel D, Chan-Ling TL, Stone J. Structure of the macroglia of the retina: sharing and division of labour between astrocytes and Müller cells. *J Comp Neurol* 1991;313(4):587-603.
 - 5 Yamada E. Some structural features of the fovea centralis in the human retina. *Arch Ophthalmol* 1969;82(2):151-159.
 - 6 Gass JD. Müller cell cone, an overlooked part of the anatomy of the fovea centralis: hypotheses concerning its role in the pathogenesis of macular hole and foveomacular retinoschisis. *Arch Ophthalmol* 1999;117(6):821-823.
 - 7 Syrbe S, Kuhrt H, Gärtner U, Habermann G, Wiedemann P, Bringmann A, Reichenbach A. Müller glial cells of the primate foveola: an electron microscopical study. *Exp Eye Res* 2018;167:110-117.
 - 8 Yoshimura N, Hangai M. *OCT atlas*. Berlin, Heidelberg: Springer Berlin Heidelberg, 2014.
 - 9 Antcliff RJ, Hussain AA, Marshall J. Hydraulic conductivity of fixed retinal tissue after sequential excimer laser ablation: barriers limiting fluid distribution and implications for cystoid macular edema. *Arch Ophthalmol Chic Ill* 2001;119(4):539-544.
 - 10 Bringmann A, Reichenbach A, Wiedemann P. Pathomechanisms of cystoid macular edema. *Ophthalmic Res* 2004;36(5):241-249.
 - 11 Govetto A, Sarraf D, Hubschman JP, Tadayoni R, Couturier A, Chehaibou I, Au A, Grondin C, Virgili G, Romano MR. Distinctive mechanisms and patterns of exudative versus tractional intraretinal cystoid spaces as seen with multimodal imaging. *Am J Ophthalmol* 2020;212:43-56.
 - 12 Tso MO. Pathological study of cystoid macular oedema. *Trans Ophthalmol Soc U K* 1980;100(3):408-413.
 - 13 Ishida S, Yamazaki K, Shinoda K, Kawashima S, Oguchi Y. Macular hole retinal detachment in highly myopic eyes: ultrastructure of surgically removed epiretinal membrane and clinicopathologic correlation. *Retina* 2000;20(2):176-183.
 - 14 Panozzo G, Mercanti A. Optical coherence tomography findings in myopic traction maculopathy. *Arch Ophthalmol* 2004;122(10):1455-1460.
 - 15 Sayanagi K, Ikuno Y, Tano Y. Tractional internal limiting membrane detachment in highly myopic eyes. *Am J Ophthalmol* 2006;142(5):850-852.
 - 16 Fujimoto M, Hangai M, Suda, Yoshimura N. Features associated with foveal retinal detachment in myopic macular retinoschisis. *Am J Ophthalmol* 2010;150(6):863-870.
 - 17 Gomaa AR, Abouhoussein MA. Optical coherence tomography findings in high myopia. *Egypt Retina J* 2013;1(2):13-17.
 - 18 Ceklic L, Munk MR, Wolf-Schnurrbusch U, Gekkieva M, Wolf S. Visual acuity outcomes of ranibizumab treatment in pathologic myopic eyes with macular retinoschisis and choroidal neovascularization. *Retina* 2017;37(4):687-693.
 - 19 AttaAllah HR, Omar IAN, Abdelhalim AS. Assessment of posterior segment using spectral domain OCT in highly myopic eyes. *Open Ophthalmol J* 2017;11:334-345.
 - 20 Fortune B, Ma KN, Gardiner SK, Demirel S, Mansberger SL. Peripapillary retinoschisis in glaucoma: association with progression and OCT signs of Müller cell involvement. *Invest Ophthalmol Vis Sci* 2018;59(7):2818-2827.
 - 21 Polk TD, Gass JD, Green WR, Novak MA, Johnson MW. Familial internal limiting membrane dystrophy. A new sheen retinal dystrophy. *Arch Ophthalmol* 1997;115(7):878-885.
 - 22 Franco-Cardenas V, Dalma-Weiszhausz J, Martinez-Munoz R, Dalma A. SD-OCT progressive alterations in a family affected with Müller cell sheen dystrophy. *Invest Ophthalmol Vis Sci* 2013;54(15):5921.
 - 23 Renner AB, Radeck V, Kellner U, Jägle H, Helbig H. Ten-year follow-up of two unrelated patients with Müller cell sheen dystrophy and first report of successful vitrectomy. *Doc Ophthalmol* 2014;129(3):191-202.
 - 24 Hikichi T, Fujio N, Akiba J, Azuma Y, Takahashi M, Yoshida A. Association between the short-term natural history of diabetic macular edema and the vitreomacular relationship in type II diabetes mellitus. *Ophthalmology* 1997;104(3):473-478.
 - 25 Bringmann A, Unterlauff JD, Wiedemann R, Barth T, Rehak M, Wiedemann P. Two different populations of Müller cells stabilize the structure of the fovea: an optical coherence tomography study. *Int Ophthalmol* 2020;40(11):2931-2948.
 - 26 Henrich PB, Monnier CA, Halfter W, Haritoglou C, Strauss RW, Lim RY, Loparic M. Nanoscale topographic and biomechanical studies of the human internal limiting membrane. *Invest Ophthalmol Vis Sci* 2012;53(6):2561-2570.
 - 27 Govetto A, Bhavsar KV, Virgili G, Gerber MJ, Freund KB, Curcio CA, Burgoyne CF, Hubschman JP, Sarraf D. Tractional abnormalities of the central foveal bouquet in epiretinal membranes: clinical spectrum and pathophysiological perspectives. *Am J Ophthalmol* 2017;184:167-180.
 - 28 Govetto A, Hubschman JP, Sarraf D, Figueroa MS, Bottoni F, dell'Omo R, Curcio CA, Seidenari P, Delle Donne G, Gunzenhauser R, Ferrara M, Au A, Virgili G, Scialdone A, Repetto R, Romano MR. The role of Müller cells in tractional macular disorders: an optical coherence tomography study and physical model of mechanical force transmission. *Br J Ophthalmol* 2020;104(4):466-472.
 - 29 Woon WH, Greig D, Savage MD, Wilson MC, Grant CA, Mokete B, Bishop F. Movement of the inner retina complex during the development of primary full-thickness macular holes: implications for hypotheses of pathogenesis. *Graefes Arch Clin Exp Ophthalmol* 2015;253(12):2103-2109.
 - 30 Bringmann A, Unterlauff JD, Wiedemann R, Rehak M, Wiedemann P. Morphology of partial-thickness macular defects: presumed roles of Müller cells and tissue layer interfaces of low mechanical stability. *Int J Retina Vitreous* 2020;6:28.

- 31 Yokota R, Hirakata A, Hayashi N, Hirota K, Rii T, Itoh Y, Orihara T, Inoue M. Ultrastructural analyses of internal limiting membrane excised from highly myopic eyes with myopic traction maculopathy. *Jpn J Ophthalmol* 2018;62(1):84-91.
- 32 Hubschman JP, Govetto A, Spaide RF, Schumann R, Steel D, Figueroa MS, Sebag J, Gaudric A, Staurengi G, Haritoglou C, Kadosono K, Thompson JT, Chang S, Bottoni F, Tadayoni R. Optical coherence tomography-based consensus definition for lamellar macular hole. *Br J Ophthalmol* 2020;104(12):1741-1747.
- 33 Bando H, Ikuno Y, Choi JS, Tano Y, Yamanaka I, Ishibashi T. Ultrastructure of internal limiting membrane in myopic foveoschisis. *Am J Ophthalmol* 2005;139(1):197-199.
- 34 Bringmann A, Iandiev I, Pannicke T, Wurm A, Hollborn M, Wiedemann P, Osborne NN, Reichenbach A. Cellular signaling and factors involved in Müller cell gliosis: neuroprotective and detrimental effects. *Prog Retin Eye Res* 2009;28(6):423-451.
- 35 Lu YB, Iandiev I, Hollborn M, Körber N, Ulbricht E, Hirrlinger PG, Pannicke T, Wei EQ, Bringmann A, Wolburg H, Wilhelmsson U, Pekny M, Wiedemann P, Reichenbach A, Käs JA. Reactive glial cells: increased stiffness correlates with increased intermediate filament expression. *FASEB J* 2011;25(2):624-631.
- 36 Kritzenberger M, Junglas B, Framme C, Helbig H, Gabel VP, Fuchshofer R, Tamm ER, Hillenkamp J. Different collagen types define two types of idiopathic epiretinal membranes. *Histopathology* 2011;58(6):953-965.
- 37 Otani T, Yamaguchi Y, Kishi S. Correlation between visual acuity and foveal microstructural changes in diabetic macular edema. *Retina* 2010;30(5):774-780.
- 38 Lu YB, Franze K, Seifert G, Steinhäuser C, Kirchhoff F, Wolburg H, Guck J, Janmey P, Wei EQ, Käs J, Reichenbach A. Viscoelastic properties of individual glial cells and neurons in the CNS. *Proc Natl Acad Sci U S A* 2006;103(47):17759-17764.
- 39 Ikeda T, Nakamura K, Oku H, Horie T, Kida T, Takai S. Immunohistological study of monkey foveal retina. *Sci Rep* 2019;9(1):5258.